

## Surface-enhanced Raman spectroscopy and correlated scanning electron microscopy of individual carbon nanotubes

Rajay Kumar, Hao Zhou, and Stephen B. Cronin

Citation: [Applied Physics Letters](#) **91**, 223105 (2007); doi: 10.1063/1.2816905

View online: <http://dx.doi.org/10.1063/1.2816905>

View Table of Contents: <http://scitation.aip.org/content/aip/journal/apl/91/22?ver=pdfcov>

Published by the [AIP Publishing](#)

---

### Articles you may be interested in

[Enhanced field emission from lanthanum hexaboride coated multiwalled carbon nanotubes: Correlation with physical properties](#)

*J. Appl. Phys.* **116**, 164309 (2014); 10.1063/1.4898352

[Enhanced field emission from cerium hexaboride coated multiwalled carbon nanotube composite films: A potential material for next generation electron sources](#)

*J. Appl. Phys.* **115**, 094302 (2014); 10.1063/1.4866990

[Synthesis of silver particles on copper substrates using ethanol-based solution for surface-enhanced Raman spectroscopy](#)

*AIP Advances* **4**, 031324 (2014); 10.1063/1.4868370

[Plasmon-induced optical field enhancement studied by correlated scanning and photoemission electron microscopy](#)

*J. Chem. Phys.* **138**, 154701 (2013); 10.1063/1.4799937

[Effect of TiO<sub>2</sub> nanoparticles on the thermal properties of decorated multiwall carbon nanotubes: A Raman investigation](#)

*J. Appl. Phys.* **108**, 083501 (2010); 10.1063/1.3496671

---

The advertisement features a photograph of the Model PS-100 cryogenic probe station, a complex piece of scientific equipment with various lenses, mirrors, and mechanical components. The background is a gradient of blue. The text is arranged around the image: 'Model PS-100' in large bold letters, 'Tabletop Cryogenic Probe Station' below it, the 'Lake Shore CRYOTRONICS' logo to the right, and the slogan 'An affordable solution for a wide range of research' at the bottom right.

**Model PS-100**  
Tabletop Cryogenic  
Probe Station

**Lake Shore**  
CRYOTRONICS

*An affordable solution for  
a wide range of research*

# Surface-enhanced Raman spectroscopy and correlated scanning electron microscopy of individual carbon nanotubes

Rajay Kumar

*Ming Hsieh Department of Electrical Engineering, University of Southern California, Los Angeles, California 90089, USA*

Hao Zhou

*Department of Physics and Astronomy, University of Southern California, Los Angeles, California 90089, USA*

Stephen B. Cronin<sup>a)</sup>

*Ming Hsieh Department of Electrical Engineering, University of Southern California, Los Angeles, California 90089, USA*

(Received 2 October 2007; accepted 1 November 2007; published online 27 November 2007)

Raman spectra of individual carbon nanotubes are measured by scanning a focused laser spot (0.5  $\mu\text{m}$  diameter) over a large area (100  $\mu\text{m}^2$ ) before and after depositing silver nanoparticles. Local regions exhibiting surface enhanced Raman spectroscopy (SERS) were located with respect to a lithographically patterned grid, allowing subsequent scanning electron microscopy to be performed. The uniquely large aspect ratio of carbon nanotubes enables imaging of the nanoparticle geometry together with the SERS active molecule. By measuring the same individual carbon nanotube before and after metal nanoparticle deposition, the SERS enhancement factor is determined unambiguously. The data reveals SERS enhancement factors up to 134 000, a consistent upshift in the *G* band Raman frequency and nanoparticle heating in excess of 600 °C.

© 2007 American Institute of Physics. [DOI: 10.1063/1.2816905]

Raman spectroscopy is a powerful tool that gives the precise vibrational energies of molecules, which provide the fingerprint for unique chemical identification. As such, Raman spectroscopy is extremely useful for a vast number of applications. However, the Raman scattering cross section of most molecules is extremely small, which generally limits its potential uses. Surface-enhanced Raman spectroscopy (SERS) can be used to improve the small Raman intensities, thus, making Raman spectroscopy related applications more practical. Reports of SERS enhancement factors span a wide range from two orders of magnitude<sup>1</sup> to fourteen orders of magnitude.<sup>2</sup> Since this previous work primarily involved nanoparticles in solution and roughened metal surfaces, it is not possible to image the exact geometry of the nanoparticle/molecule complex. Consequently, several unexplored factors remain, including the separation between the nanoparticle and Raman active molecule, the number of molecules on each nanoparticle, the number of nanoparticles within the focal volume, and the extent to which nanoparticles couple plasmonically to each other. A more complete understanding of SERS will enable reliable single molecule spectroscopy and bring forth applications and analytical techniques achievable with handheld spectrometers.

Kneipp *et al.* obtained SERS enhancement factors of  $10^{14}$  using colloidal silver nanoparticles by correlating the SERS intensity of a single molecule to an equivalent intensity derived from  $10^{14}$  nonenhanced molecules.<sup>2</sup> In another experiment, a 10  $\mu\text{m}$  diameter bundle of nanotubes, in contact with a silver nanoparticle cluster, exhibited an enhanced anti-Stokes *G* band due to vibrational pumping from the extremely high electric fields of the nanoparticles.<sup>3</sup> Measure-

ments of DNA with controlled interparticle spacing of bound gold nanoparticles have yielded  $10^3$ – $10^6$ -fold enhancements in Raman intensity.<sup>4</sup> Three-dimensional nanocrescents, nanoshells, and nanorods have also demonstrated Raman enhancement capabilities.<sup>5–7</sup> Attempts to explain this phenomenon with classical electrodynamics indicate that particle proximity, surface roughness, and nanoparticle size all contribute to the SERS effect.<sup>5,8,9</sup> Atomic force microscopy and scanning electron microscopy (SEM) studies of bulk samples, where roughness and nanoparticle size are varied, have been performed to further understand the SERS effect.<sup>10</sup> Though offering interesting results, these experiments reveal general characteristics of large ensembles but offer little information about the individual nanoparticles and molecules involved in the SERS process.

In this work, we conduct a systematic study of SERS on individual carbon nanotubes. A focused laser spot is scanned over the sample to identify SERS “hot spots.” The geometry of both the metal nanoparticles and carbon nanotubes at a given hot spot are imaged using SEM. Raman spectra taken before and after depositing nanoparticles are used to determine the enhancement factor of the SERS hot spot region. In this scheme, the carbon nanotubes serve as Raman active molecules to study the SERS phenomenon. Unlike most single molecules, the uniquely large aspect ratio and conducting properties of carbon nanotubes allow them to be imaged by SEM. Burnout of these robust molecules allows quantification of the heat generated by the SERS plasmonic phenomenon.

Nanotubes are grown by chemical vapor deposition (CVD) from iron (III) nitrate catalyst nanoparticles in methane gas at 900 °C for 10 min on a Si/SiO<sub>2</sub> substrate.<sup>11</sup> A numbered grid is patterned on the substrate using electron-beam lithography. This grid allows the laser spot to be

<sup>a)</sup>Electronic mail: scronin@usc.edu

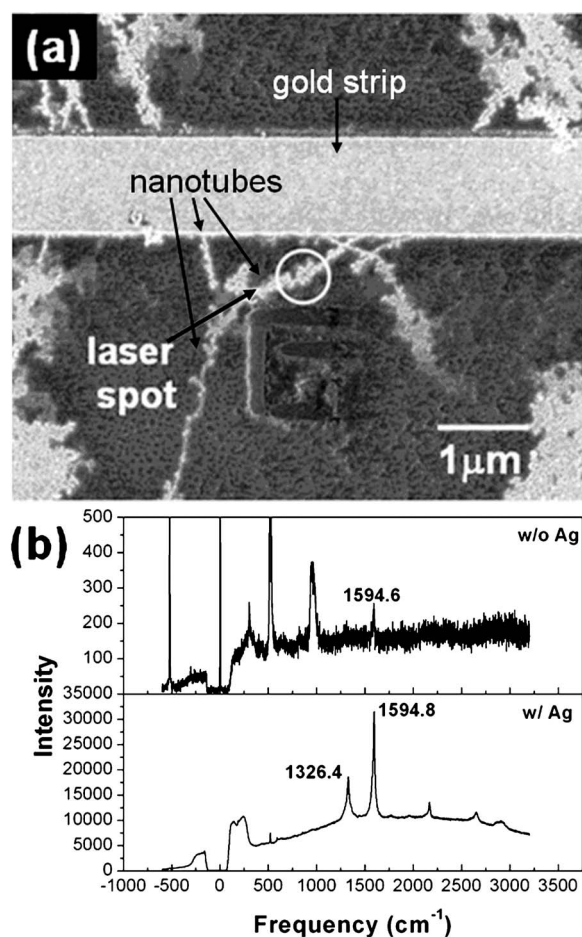


FIG. 1. (a) SEM image of carbon nanotubes covered with a film of Ag nanoparticles. The white circle indicates the size and location of the laser spot. (b) Raman spectra taken at the laser spot position indicated in (a) before and after Ag deposition.

aligned optically with a single isolated carbon nanotube. A 6 nm thick film of Ag is deposited on the entire sample area in an electron-beam metal evaporator at a pressure of  $5 \times 10^{-7}$  Torr. Since a 6 nm deposition of Ag is not enough to form a complete continuous film, nanometer-sized islands are formed, which serve as the SERS enhancing nanoparticles. Typical nanoparticle sheet densities are  $\sim 2500/\mu\text{m}^2$  for a 6 nm thick Ag film.<sup>12</sup> Though the plasmon resonance of silver lies in the ultraviolet wavelength range, it is shifted into the visible spectrum due to the nanoparticle geometry.<sup>13</sup> Raman spectra are taken with a Renishaw inVia Reflex micro-Raman spectrometer using a  $100\times$  objective lens with a  $0.5 \mu\text{m}$  spot size. Employing a high precision automated microscope stage (Prior, Inc.), local spectra were taken over several hundred square micrometers on the fiducial grid. Spectra were collected at the locations of approximately 100 nanotubes before and after depositing silver nanoparticles. Only those nanotubes exhibiting a finite Raman signal before and after are reported here.

Figure 1 shows a SEM image of CVD grown nanotubes coated with Ag nanoparticles and lithographically defined features that allow correlation between microscopy and spectroscopy. The nanotubes and gold strip appear bright in the SEM image due to the electron beam induced charge contrast.<sup>14</sup> As a consequence of this contrast, only the Ag nanoparticles touching carbon nanotubes appear bright, even though the entire sample is coated uniformly with nanopar-

TABLE I. SERS related effects of five carbon nanotubes.

Nanotube	G band frequency upshift ( $\Delta\omega_G$ ) ( $\text{cm}^{-1}$ )	Raman intensity ratio ( $I_{\text{SERS}}/I_0$ )	SERS enhancement factor
1	0.2	335	134 000
2	5.8	195	78 000
3	0.2	38	15 200
4	5.1	8.6	3440
5	4.3	27	10 800

ticles. Similarly, only those nanotubes that are in contact with the lithographically patterned gold strip appear bright.

The two Raman spectra in Fig. 1(b) were collected from the “laser spot” region indicated in the SEM image, before and after depositing Ag nanoparticles. Both spectra were collected at the same location with a 120 s integration time using a 633 nm laser at 2 mW. G band Raman spectra were fit using a mixed Lorentzian/Gaussian line shape after subtracting a linear baseline. Before depositing the Ag nanoparticles, the G band Raman mode, appearing at  $1594.6 \text{ cm}^{-1}$ , shows an intensity of 58 photon counts. After depositing the Ag nanoparticles, the G band intensity reaches 19 450 photon counts. This factor of 335 enhancement is due to the surface plasmon resonance of the Ag nanoparticles, which couples the incident light into the nanotube very effectively. Several major silicon peaks from the underlying substrate can be seen at 303, 520, and  $1000 \text{ cm}^{-1}$  and have not undergone an increase in intensity. Also, the spectrum taken with Ag nanoparticles exhibits a broad background due to luminescence from the Ag nanoparticles.

The SERS enhancement factors of five nanotubes were measured in this fashion and are listed in Table I. Three of the five nanotubes measured in this study show a significant upshift in the G band frequency after the deposition of Ag nanoparticles. We also observed upshifts in the radial breathing mode (RBM), D band, and G' band Raman peaks. In most cases, the RBM, D band, and G' band only appear in the SERS spectra due to the weak Raman signals of the pristine nanotubes. Possible reasons for these upshifts are charge transfer from the metal nanoparticles to the nanotubes and surface pressure exerted on the nanotubes by the Ag nanoparticles.<sup>15,16</sup> The nanotubes' high surface-to-volume ratios make their Raman spectra extremely sensitive to slight modifications of their surface. The Raman spectra of nanotubes have been shown to upshift as free charge is increased.<sup>17,18</sup> Mechanical pressure is also known to increase the vibrational frequency of carbon nanotubes.<sup>15,19,20</sup> According to the work of Venkateswaran *et al.*,<sup>15</sup> a  $3 \text{ cm}^{-1}$  upshift of the G band corresponds to a pressure of 0.5 GPa.<sup>15</sup> While these extremely high pressures may seem unlikely, surface forces on the nanometer scale have been shown to exert pressures of this magnitude.<sup>21</sup>

In our measurements, we observe enhancements in the Raman intensity ratio ( $I_{\text{SERS}}/I_0$ ) up to 335 measured from nanotubes with a  $0.5 \mu\text{m}$  diameter laser spot. Although the number of Ag nanoparticles in the  $0.5 \mu\text{m}$  laser spot is approximately 490, it is likely that the SERS enhanced signal originates from the location of only one nanoparticle or between two nanoparticles and hence a 25 nm or shorter segment of the nanotube. We infer this is true because of the sheer rarity of finding a SERS hot spot and the large strength

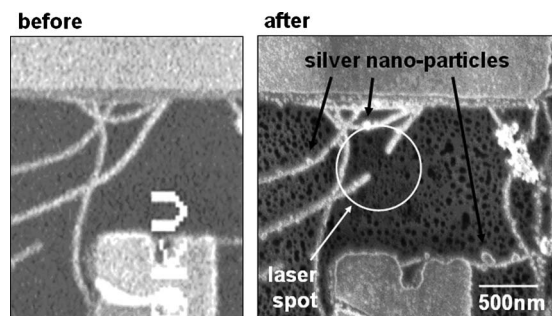


FIG. 2. SEM images of a nanotube before and after Ag nanoparticle deposition and SERS-induced burnout.

of the Raman signal when they were found. In this case, the SERS-active region is at most 25 nm in size, which gives an effective area that is 400 times smaller than the 500 nm diameter laser spot. Thus, the true enhancement factor is 400 times larger than the intensity ratio from the measured spectra, giving our intensity ratio of 335 a total SERS enhancement factor of 134 000, as indicated in Table I. The reason for taking the ratio of the areas  $[(25 \text{ nm})^2 / (500 \text{ nm})^2]$  instead of the lengths  $(25 \text{ nm} / 500 \text{ nm})$  is that these length scales are much smaller than the wavelength of light. Therefore, a photon passing 20 nm away from a nanotube can still be absorbed (or scattered). It is, therefore, important to include the area of the SERS enhanced volume, rather than just the length, in determining the SERS enhancement factor.

The plasmonic charge oscillating on the surface of the Ag nanoparticles causes Joule-like heating in the nanoparticles, producing elevated temperatures. Figure 2 shows SEM images of a nanotube before and after being burned out by these high temperatures. Since it is known that nanotubes burn out in air above 600 °C,<sup>22–24</sup> the results shown in Fig. 2 demonstrate that Ag nanoparticles can reach temperatures in excess of 600 °C when irradiated with laser powers of 20 mW. We observed this SERS-induced burnout in a total of three nanotubes. It should also be noted that all of the nanotubes shown in these SEM images were irradiated with 20 mW of laser light. However, only the SERS-active region exhibited burnout, further demonstrating the spatial rarity of such an event. The three nanotubes exhibiting burnout were from a different set of nanotubes than those shown in Fig. 1 and Table I, which were not exposed to laser powers above 2 mW. Furthermore, Raman spectra taken from these burnt out nanotubes were not taken before adding the Ag nanoparticles. Therefore, no correlation between burnout threshold and SERS enhancement factor could be made.

Oubre *et al.* performed finite-difference time-domain (FDTD) simulations to model the SERS effects of two nearly touching metallic nanoshells irradiated with laser light.<sup>25</sup> Though our experiments use solid nonspherical nanoparticles, they are resonant with 633 nm wavelength laser light and have been found to be qualitatively similar to metallic nanoshells in similar experiments.<sup>26</sup> These FDTD simulations show that nanoshells spaced 1.5 nm apart will have a SERS enhancement three orders of magnitude higher than that of individual nanoshells.<sup>25</sup> The maximum enhancement occurs in a small region in between the nanoshells and decays quickly away from this region.<sup>25</sup> For the randomly distributed nanoparticles in our study, the probability is extremely low that two very closely spaced nanoparticles will

lay on either side of a carbon nanotube. Our measurements show that the occurrence rate of SERS hot spots is very low, which reflects the small effective volume of SERS enhancement. In the future, more effective techniques for generating SERS that make better use of the nanoparticle geometry will improve the probability of this rare event and enable related applications.

In conclusion, the SERS enhancement of individual carbon nanotubes is measured through the use of correlated micro-Raman spectroscopy. A fiducial grid enables the ability to obtain Raman spectra and SEM images of carbon nanotubes before and after the deposition of silver nanoparticles. The Raman intensity of carbon nanotubes was observed to increase 134 000-fold through the SERS phenomenon. The localized burnout of nanotubes in SERS hot spot regions is attributed to the heat dissipated by the immense plasmonic charge oscillating in the Ag nanoparticles.

- <sup>1</sup>K. Kneipp, G. Hinzmann, and D. Fassler, *J. Mol. Liq.* **29**, 197 (1984).
- <sup>2</sup>K. Kneipp, Y. Wang, H. Kneipp, L. T. Perelman, I. Itzkan, R. R. Dasari, and M. S. Feld, *Phys. Rev. Lett.* **78**, 1667 (1997).
- <sup>3</sup>K. Kneipp, H. Kneipp, P. Corio, S. D. M. Brown, K. Shafer, J. Motz, L. T. Perelman, E. B. Hanlon, A. Marucci, G. Dresselhaus, and M. S. Dresselhaus, *Phys. Rev. Lett.* **84**, 3470 (2000).
- <sup>4</sup>L. A. Gearheart, H. J. Ploehn, and C. J. Murphy, *J. Phys. Chem. B* **105**, 12609 (2001).
- <sup>5</sup>G. L. Liu, Y. Lu, J. Kim, J. C. Doll, and L. P. Lee, *Adv. Mater. (Weinheim, Ger.)* **17**, 2683 (2005).
- <sup>6</sup>Y. Yang, L. Xiong, J. Shi, and M. Nogami, *Nanotechnology* **17**, 2670 (2006).
- <sup>7</sup>M. Suzuki, Y. Nidome, N. Terasaki, K. Inoue, Y. Kuwahara, and S. Yamada, *Jpn. J. Appl. Phys., Part 2* **43**, L554 (2004).
- <sup>8</sup>H. Xu, J. Aizpurua, M. Käll, and P. Apell, *Phys. Rev. E* **62**, 4318 (2000).
- <sup>9</sup>F. J. Garcia-Vidal and J. B. Pendry, *Phys. Rev. Lett.* **77**, 1163 (1996).
- <sup>10</sup>R. M. Stöckle, V. Deckert, C. Fokas, and R. Zenobi, *Appl. Spectrosc.* **54**, 1577 (2000).
- <sup>11</sup>J. Kong, H. T. Soh, A. M. Cassell, C. F. Quate, and H. J. Dai, *Nature (London)* **395**, 878 (1998).
- <sup>12</sup>S. E. Roark, D. J. Semin, and K. L. Rowen, *Anal. Chem.* **68**, 473 (1996).
- <sup>13</sup>J. Okumu, C. Dahmen, A. N. Sprafke, M. Luysberg, G. von Plessen, and M. Wuttig, *J. Appl. Phys.* **97**, 094305 (2005).
- <sup>14</sup>T. Brintlinger, Y.-F. Chen, T. Dürkop, E. Cobas, M. S. Fuhrer, J. D. Barry, and J. Meingailis, *Appl. Phys. Lett.* **81**, 2454 (2002).
- <sup>15</sup>U. D. Venkateswaran, E. A. Brandson, U. Schlecht, A. M. Rao, E. Richter, I. Loa, K. Syassen, and P. C. Eklund, *Phys. Status Solidi B* **223**, 225 (2001).
- <sup>16</sup>S. Lefrant, J. P. Buisson, J. Schreiber, O. Chauvet, M. Baibarac, and I. Baltog, *Synth. Met.* **139**, 783 (2003).
- <sup>17</sup>S. B. Cronin, R. Barnett, M. Tinkham, S. G. Chou, O. Rabin, M. S. Dresselhaus, A. K. Swan, M. S. Ünlü, and B. B. Goldberg, *Appl. Phys. Lett.* **84**, 2052 (2004).
- <sup>18</sup>P. Corio, P. S. Santos, V. W. Brar, G. G. Samsonidze, S. G. Chou, and M. S. Dresselhaus, *Chem. Phys. Lett.* **370**, 675 (2003).
- <sup>19</sup>S. Reich, C. Thomsen, and J. Maultzsch, *Carbon Nanotubes: Basic Concepts and Physical Properties* (Wiley-VCH, Weinheim, Germany, 2004), Chap. 6.2, pp. 107–111.
- <sup>20</sup>R. Kumar and S. B. Cronin, “Raman spectroscopy of Carbon Nanotubes Under Axial Strain,” *J. Nanosci. Nanotechnol.* (to be published).
- <sup>21</sup>S. B. Cronin, A. K. Swan, M. S. Ünlü, B. B. Goldberg, M. S. Dresselhaus, and M. Tinkham, *Phys. Rev. Lett.* **94**, 167401 (2004).
- <sup>22</sup>F. Cataldo, Fullerenes, Nanotubes, Carbon Nanostruct. **10**, 293 (2002).
- <sup>23</sup>I. W. Chiang, B. E. Brinson, A. Y. Huang, P. A. Willis, M. J. Bronikowski, J. L. Margrave, R. E. Smalley, and R. H. Hauge, *J. Phys. Chem. B* **105**, 8297 (2001).
- <sup>24</sup>K. Hata, D. N. Futaba, K. Mizuno, T. Namai, M. Yumura, and S. Iijima, *Science* **306**, 1362 (2004).
- <sup>25</sup>C. Oubre and P. Nordlander, *J. Phys. Chem. B* **109**, 10042 (2005).
- <sup>26</sup>P. Nordlander, C. Oubre, E. Prodan, K. Li, and M. I. Stockman, *Nano Lett.* **4**, 899 (2004).